

## ELASTIC SCATTERING OF X-RAYS AND $\Gamma$ -RAYS BY $2s$ ELECTRONS IN IONS AND NEUTRAL ATOMS\*

K. KARIM<sup>1</sup>, M. L. MUNTEANU<sup>1</sup>, S. SPÂNULESCU<sup>1,2</sup>, C. STOICA<sup>1</sup>

<sup>1</sup>University of Bucharest, Department of Physics, MG11, Bucharest-Magurele 077125, Romania

<sup>2</sup>“Hyperion” University of Bucharest, Department of Physics, Bucharest 030629, Romania

Received October 17, 2011

*Abstract.* A dynamic screening model based on nonrelativistic Hartree-Fock approach is given for the  $2s$  subshell Rayleigh scattering amplitudes and the total photoeffect cross-section. It considerably improves the predictions for low atomic number elements especially in a large energy range starting from one and half the photoeffect threshold energy. A good agreement with full relativistic numerical calculations is observed for these elements and energies also.

*Key words:* dynamic screening model, elastic scattering, X-rays and  $\Gamma$ -rays.

### 1. INTRODUCTION

Since long time ago the subject of X-rays and  $\Gamma$ -rays scattering by inner shell electrons in atoms has presented a large interest. Experimental and theoretical advances have allowed a continuous progress in this topic, the results of such investigations being useful in many fields such as laser thermonuclear fusion, plasma physics, lasers, astrophysics and others. As important experimental progress, we want to mention the creation of the X-ray free electron laser with high spectral resolution [1, 2, 3], while as theoretical results we mention the works [4–10]. Usually the term inner shell electrons is used to describe in a fairly good approximation electrons whose quantum states given by wave functions, energies, orbital kinetic moment etc. are perturbed very little by the interactions with the other electrons in the atom. More specific, it is realistic to consider that K-shell and L-shell electrons may be described by hydrogen-like wave functions and energies with an appropriate effective charge  $Z_{eff}$ . In such a way, photon scattering by  $1s$  and  $2s$  bound electrons may be described by analytical formulae which give precise numerical predictions. Further, it is realistic to consider that inner electrons hydrogen-like quantum states are less perturbed by interatomic interactions in molecules and solids.

\* Paper presented at the Annual Scientific Session of Faculty of Physics, University of Bucharest, June 17, 2011, Bucharest-Magurele, Romania.

It has been proven [8–10] that the Coulombian shape of inner  $1s$  and  $2s$  electrons wave functions with an effective charge  $Z_{eff}$  obtained by fitting the Hartree-Fock charge distribution with the Coulombian one is a good approach which gives very good predictions for Rayleigh and photoeffect cross-sections. As expected, this simple screening model is especially good in the case of large atomic numbers  $Z$  (when the interaction of the inner electron with the nucleus is strong) and far enough from the photoeffect threshold (at least one and a half the photoeffect threshold energy). In this paper we are able to improve our screening model considering a dynamic screening constant, *i.e.* in the case of large photon energies the effective charge is the same for a large energy range as it is given by the Hartree-Fock calculations, but below twice the ionization energy we consider that  $Z_{eff}$  decreases linearly till a threshold value  $Z_{eff}^{th}$  given by the experimental

threshold energy  $\omega_{2s}^{th} = [1 - \varepsilon(Z_{eff}^{th})]m$ , where  $\varepsilon(Z) = \left( \frac{1 + \sqrt{1 - \alpha^2 Z^2}}{2} \right)^{1/2}$ . Thus

we follow the same approach that we used in a previous paper [11] in the case of Rayleigh scattering by K-shell electrons. We want to mention that in the case of  $2s$  electrons, the screening model must be considered in a more subtle way, because the effective charge variation is significantly larger than in the K-shell case and the charge distribution spans a larger range.

## 2. THE DYNAMIC SCREENING MODEL FOR RAYLEIGH SCATTERING AND PHOTOEFFECT FOR THE $2s$ SUBSHELL

The Kramers-Heisenberg-Waller (KHW) matrix element for the two-photon elastic scattering may be written in the second order of the perturbation theory as:

$$\mathcal{M} = M(\Omega_1) + M(\Omega_2), \quad (1)$$

where

$$\Omega_1 = \omega + E_{2s} + i\varepsilon, \quad \Omega_2 = -\omega + E_{2s} - i\varepsilon, \quad (2)$$

$$M(\Omega_1) = -m \lim_{\varepsilon \rightarrow 0} \sum_n \frac{\langle i | e^{-ik_2 \cdot \vec{r}_2} (\vec{\alpha} \cdot \vec{s}_2) | n \rangle \langle n | e^{ik_1 \cdot \vec{r}_1} (\vec{\alpha} \cdot \vec{s}_1) | i \rangle}{E_n - (\omega + E_{2s} + i\varepsilon)}, \quad (3)$$

$$M(\Omega_2) = -m \lim_{\varepsilon \rightarrow 0} \sum_n \frac{\langle i | e^{ik_1 \cdot \vec{r}_2} (\vec{\alpha} \cdot \vec{s}_1) | n \rangle \langle n | e^{-ik_2 \cdot \vec{r}_1} (\vec{\alpha} \cdot \vec{s}_2) | i \rangle}{E_n - (-\omega + E_{2s} - i\varepsilon)},$$

and  $\omega, \vec{k}_j = \omega \vec{v}, \vec{s}_j$  are the energy, momentum and polarisation of the incident ( $j=1$ ) and scattered ( $j=2$ ) photons. The energy of the initial state of the target electron, which is the same as the final state, meaning the  $2s_{1/2}$  Dirac state in coulombian field is  $E_{2s} = m\sqrt{\frac{1+\gamma}{2}}$  with  $\gamma = (1 - \alpha^2 Z^2)^{1/2}$ .

The sum over the complete set of intermediate  $|n\rangle$  implies both negative and positive frequencies contributions. The  $\vec{\alpha} \cdot \vec{s}$  operator is expressed in terms of the Dirac 4x4 matrices. The quantity  $\varepsilon > 0$ , arbitrary small, allows avoiding the singularities when

$$E_n = \omega + E_{2s} \text{ or } E_n = -\omega + E_{2s}. \quad (4)$$

Following the procedure presented in some previous papers [7, 8, 10], we could obtain the nonrelativistic limit of the Rayleigh amplitudes in terms of the invariant amplitudes

$$\mathcal{M} = M(\omega, \theta)(\vec{s}_1 \cdot \vec{s}_2) + N(\omega, \theta)(\vec{s}_1 \cdot \vec{v}_2)(\vec{s}_2 \cdot \vec{v}_1). \quad (5)$$

The differential cross section of the Rayleigh scattering (per  $2s$  electron) for unpolarized photons is

$$\frac{d\sigma}{d\Omega} = \frac{r_0^2}{2} (|A_\perp|^2 + |A_\parallel|^2), \quad (6)$$

where

$$A_\perp = M(\omega, \theta) \text{ and } A_\parallel = M(\omega, \theta)\cos\theta - N(\omega, \theta)\sin^2\theta. \quad (7)$$

The amplitudes  $M$  and  $N$  in the above formulae have been expressed in terms of the photon energy  $\omega$  and scattering angle  $\theta$  in the form

$$M(\omega, \theta) = \mathcal{O}(\theta) - P(\Omega_1, \theta) - P(\Omega_2, \theta) \quad (8)$$

and

$$N(\omega, \theta) = -[Q(\Omega_1, \theta) + Q(\Omega_2, \theta)]. \quad (9)$$

In these relationships, the nonrelativistic limit of the various terms involved for the  $2s$  subshell have specific expressions that we present in the following.

Thus, the nonrelativistic atomic form factor for the  $2s$  subshell was found as

$$\mathcal{O}(\theta) = \frac{1}{2} \frac{1}{\left(1 + \frac{\delta^2}{4}\right)^{1+\gamma}} \left\{ \frac{\sin(\gamma\phi) \cos(\gamma\phi)}{\gamma \sin\phi \cos\phi} + \cos[(2\gamma+2)\phi] - \frac{\delta}{4\varepsilon} \sin[(2\gamma+2)\phi] \right\}, \quad (10)$$

where

$$\delta = \frac{|\vec{k}_2 - \vec{k}_1|}{\eta} = \frac{\Delta}{\eta} = \frac{4\varepsilon\omega}{\alpha Zm} \sin \frac{\theta}{2}, \quad \phi = \arctan \frac{\delta}{2}, \quad (11)$$

and  $\vec{\Delta} = \vec{k}_2 - \vec{k}_1$  is the momentum transfer between the scattered photon and the electron while  $\eta = \alpha Zm / 2\varepsilon$  is the mean value of the momentum of the  $2s$  electron.

In the case of the  $2s$  subshell, the amplitudes involved in the previous expression have more complicated expressions than in the case of K-shell electrons, as follows

$$\begin{aligned} P(\Omega, \theta) = & 16 \frac{\lambda^5}{\varepsilon^5} \left\{ \frac{3}{2} (1-\gamma)^4 m^4 \frac{\Omega^2}{\omega^2} \delta^4 \frac{X^7}{d^8} \frac{F_1(4-\tau; 4, 4; 5-\tau; x_1, x_2)}{(4-\tau)} + \right. \\ & + \frac{X^5}{d^6} \frac{F_1(3-\tau; 3, 3; 4-\tau; x_1, x_2)}{(3-\tau)} \times \\ & \times \left[ \frac{4\eta^4}{m^2} + (1-\gamma)^2 \frac{m^2}{\omega^2} \left( \pm 2\Omega\omega + \frac{3}{8} \alpha^2 Z^2 \Omega^2 - \frac{5}{32} \alpha^4 Z^4 m^2 \right) \delta^2 \right] + \\ & + \frac{X^3}{d^4} \frac{F_1(2-\tau; 2, 2; 3-\tau; x_1, x_2)}{(2-\tau)} \times \\ & \times \left[ 1 \mp \frac{1}{4} \alpha^2 Z^2 (1-\gamma) \frac{\Omega}{\omega} \mp \frac{1}{8} \alpha^2 Z^2 (1-\gamma)^2 \frac{\Omega}{\omega} + \frac{\alpha^2 Z^2}{2} (1-\gamma) \frac{\omega_{2s}^2}{\omega^2} \right] \Big\} + \\ & + \frac{\alpha^2 Z^2}{4} \frac{m}{\varepsilon\omega} \frac{1}{\left(1 + \frac{\delta^2}{4}\right)^3} \left[ \pm 1 - \frac{1}{4} (1-\gamma)^2 \frac{\Omega}{\omega} + \frac{1}{2} \left( \pm 1 + \frac{\alpha^2 Z^2}{8} \frac{\Omega}{\omega} \right) \delta^2 \right], \end{aligned} \quad (12)$$

$$\begin{aligned} Q(\Omega, \theta) = & -3 \cdot 2^{17} \omega^2 \eta^7 m^2 (1-\gamma) \delta^2 \left[ 1 + \gamma - \frac{1-\gamma}{4\omega^2} (\gamma X^2 + \eta^2) \delta^2 \right] \times \\ & \times \frac{X^9}{d^{10}} \frac{F_1(5-\tau; 5, 5; 6-\tau; x_1, x_2)}{(5-\tau)} + \\ & + 3 \cdot 2^{14} \omega^2 \eta^7 \left\{ 4 + 3\gamma + \frac{1-\gamma}{4\omega^2} \delta^2 \left[ -X^2 (7\gamma + 2) + 2\omega^2 - 5\eta^2 + \alpha^2 Z^2 \Omega^2 \right] \right\} \times \\ & \times \frac{X^7}{d^8} \frac{F_1(4-\tau; 4, 4; 5-\tau; x_1, x_2)}{(4-\tau)} + 2^{13} \eta^5 \omega^2 \left\{ 1 - \frac{3}{8} (1-\gamma) + \frac{5}{8} \alpha^2 Z^2 \frac{X^2}{\omega^2} \pm \right. \\ & \pm \varepsilon \left[ \frac{3}{4} (1-\gamma) - \frac{\alpha^2 Z^2}{2} \right] \frac{m}{\omega} - \frac{1}{8} \alpha^2 Z^2 (1-\gamma) \frac{m^2}{\omega^2} + \frac{3}{8} \alpha^2 Z^2 (1-\gamma) \frac{X^2}{\omega^2} \Big\} \times \\ & \times \frac{X^5}{d^6} \frac{F_1(3-\tau; 3, 3; 4-\tau; x_1, x_2)}{(3-\tau)} - \left[ \frac{3}{4} \alpha^2 Z^2 \pm \frac{3}{4} \frac{\alpha^2 Z^2}{\varepsilon} \frac{\omega}{m} \mp \frac{2\omega}{m} \left( 1 + \frac{\delta^2}{4} \right) \right] \frac{1}{\left(1 + \frac{\delta^2}{4}\right)^4}, \end{aligned} \quad (13)$$

for each of the cases  $\Omega = \Omega_1$  or  $\Omega = \Omega_2$ . In the expressions above

$$d = 2(\eta^2 \mp \varepsilon m \omega + \eta X); \quad d^* = 2(\eta^2 \mp \varepsilon m \omega - \eta X),$$

while the arguments  $x_1$  and  $x_2$  of the Appell  $F_1$  functions are the roots of the equation  $x^2 - sx + u^2 = 0$ , where  $u = d^* / d$ ,  $s = 2u \left( 1 - \frac{X^2 \Delta^2}{2m^2 \omega^2} \right)$  and

$$X(\Omega) = (m^2 - \Omega^2)^{1/2}.$$

In these expressions we must consider the nonrelativistic limit of the parameter  $X$  as  $X^2(\Omega_j) = \mp 2\varepsilon m \omega + \eta^2$  and also the nonrelativistic limit of the parameter  $\tau_j = \alpha Z m / X(\Omega_j)$ .

Using the optical theorem, the total cross section of the photoeffect on the  $2s$  electrons is obtained as

$$\sigma_{2s}^{ph} = \frac{4\pi^2}{3} r_0^2 \alpha^5 Z_{ef}^6 \frac{m^3}{\omega^3} \frac{\Omega_1}{\omega} \left( 1 + \frac{3}{8} \alpha^2 Z_{ef}^2 \frac{m}{\omega} \right) \frac{e^{-\tau_1 [\pi + \chi_1(\omega)]}}{1 - e^{-2\pi|\tau_1|}} \left[ 1 - \frac{32}{5} \frac{\omega_{2s}}{\omega} \frac{\omega_{2s}}{m} \right], \quad (14)$$

where

$$\omega_{2s} = (1 - \varepsilon)m \quad (15)$$

is the threshold energy for the  $2s$  subshell and

$$\chi_1(\omega) = \begin{cases} -\pi + 2 \arctan \frac{\eta |X_1|}{-\varepsilon m \omega + \eta^2}, & \omega \leq \frac{\eta^2}{m\varepsilon} \\ \pi - 2 \arctan \frac{\eta |X_1|}{\varepsilon m \omega - \eta^2}, & \omega > \frac{\eta^2}{m\varepsilon} \end{cases} \quad (16)$$

In a previous paper [10], we noticed a very good agreement of the results obtained with these formulae, for targets with intermediate and high  $Z$ , with other relativistic calculations [12, 13] of the total photoeffect cross-section and angular distribution, if the photon energy is higher than at least one and half the photoeffect threshold energy. However, for low  $Z$  elements and energies closer to the photoeffect threshold, the limitations of the model based on a constant effective atomic charge lead to increased errors.

In order to extend these formulae to low atomic number elements and energies closer to the photoeffect threshold we propose in this paper some improvements to the previous model.

Considering that the interaction of the incident photon occurs at a distance from the nucleus proportional with the wavelength

$$r_{\text{int}} \sim \lambda \sim \frac{1}{\omega} \quad (17)$$

and taking into account that the dynamic effective atomic charge  $Z_{\text{din}}$  “seen” by the photon decreases roughly linearly with the distance, starting from the static value  $Z_{\text{st}}$

$$Z_{\text{din}} = Z_{\text{st}} - C_0 r_{\text{int}}, \quad (18)$$

we may calculate an effective atomic charge which dynamically varies with the incident photon energy as

$$Z_{\text{din}} = Z_{\text{st}} - \frac{C}{\omega}. \quad (19)$$

The static value for the effective atomic charge is obtained by fitting the Hartree-Fock wave function with a  $2s$  coulombian one, as described in [10]. The constant  $C$  may be obtained by using an iterative procedure and imposing that the variation at the last step should be less than 1%.

For low  $Z$  values the quantity  $\varepsilon = \left(\frac{1+\gamma}{2}\right)^{1/2}$  is close to unity, so that in these cases it is possible to put  $\varepsilon = 1$ . On another hand, the Independent Particle Approximation (IPA) is a poor approach near the photoeffect threshold, so that we do not expect good predictions in a range just above the threshold.

The nonrelativistic limit of the parameter  $\chi_1(\omega)$  that occurs in the exponential in eq. (14) may be written as

$$\chi_1(\omega) = \begin{cases} -\pi + 2 \arctan \frac{\eta |X_1|}{-E_{2s} \omega + \eta^2}, & \omega \leq \frac{\eta^2}{E_{2s}} \\ \pi - 2 \arctan \frac{\eta |X_1|}{E_{2s} \omega - \eta^2}, & \omega > \frac{\eta^2}{E_{2s}}, \end{cases} \quad (20)$$

where  $E_{2s} = \varepsilon m$  is the energy of the  $2s$  electron.

Using this model we obtained the numerical results for the total photoeffect cross sections in the nonrelativistic limit shown in Tables 1–4.

Table 1

The photoeffect cross-sections (barns) from the 2s electrons of calcium compared with the results of Scofield [12] at various incoming photon energy. The column  $\varepsilon$  indicates the differences of the present dynamic screening model, while the column  $\varepsilon_s$  indicates the differences of the static model in reference [10]

$\hbar\omega$ (keV)	$\sigma_{2s}^{Sco}$ (barns)	$\sigma_{2s}$ (barns)	$\varepsilon$ (%)	$\varepsilon_s$ (%)	$Z_{eff}$
2	19222	19254	0.166347	15.3637	16.07
4	4044	3904	-3.46189	2.5395	16.645
6	1498	1522.17	1.61341	-2.863	17.22
8	715	705.068	-1.38905	-5.78847	17.22
10	396	382.557	-3.39482	-7.74136	17.22
15	130	122.283	-5.93587	-10.2211	17.22
20	57.8	53.3273	-7.73823	-11.9701	17.22
30	17.74	16.1556	-8.93107	-13.1386	17.22
40	7.51	6.82678	-9.0975	-13.3135	17.22
50	3.82	3.47819	-8.94783	-13.1808	17.22
60	2.18	1.99879	-8.31225	-12.5816	17.22

Table 2

The same as in Table 1, for zinc

$\hbar\omega$ (keV)	$\sigma_{2s}^{Sco}$ (barns)	$\sigma_{2s}$ (barns)	$\varepsilon$ (%)	$\varepsilon_s$ (%)	$Z_{eff}$
2	48411	49309.7	1.85649		23.63
3	22932	22244.8	-2.99665	8.06422	24.4133
4	12865	12126	-5.74435	2.08311	24.805
6	5361	5318.65	-0.789877	-4.60344	25.98
8	2770	2643.33	-4.57292	-8.38304	25.98
10	1626	1511.21	-7.05943	-10.8816	25.98
15	591	528.247	-10.6181	-14.4747	25.98
20	279.6	244.322	-12.6173	-16.4954	25.98

Table 3

The same as in Table 1, for silver

$\hbar\omega$ (keV)	$\sigma_{2s}^{Sco}$ (barns)	$\sigma_{2s}$ (barns)	$\varepsilon$ (%)	$\varepsilon_s$ (%)	$Z_{eff}$
5	21664	20109.7	-7.17465		38.01
6	15589	14494.9	-7.01845		38.9433

Table 3 (continued)

8	8990	8372.16	-6.87249	9.57465	40.11
10	5710.6	5331.93	-6.63104	7.09927	40.81
20	1226.1	1269.43	3.53387	0.651272	43.61
30	459.6	468.018	1.83158	-1.65559	43.61
40	221.87	224.845	1.3408	-2.55894	43.61
80	34.94	35.9012	2.75096	-2.02835	43.61
100	18.838	19.5884	3.9834	-1.05172	43.61
150	6.027	6.44561	6.94555	1.47363	43.61
200	2.674	2.91872	9.15165	3.40656	43.61
300	0.8637	0.958162	10.9369	4.92662	43.61
400	0.3986	0.437464	9.75017	3.71595	43.61

Table 4

The same as in Table 1, for lead

$\hbar\omega$ (keV)	$\sigma_{2s}^{Sc}$ (barns)	$\sigma_{2s}$ (barns)	$\epsilon$ (%)	$\epsilon_s$ (%)	$Z_{eff}$
23.565	3415	3222.09	-5.64877	-1.75204	77.8083
25	3032	2888.42	-4.73556	-0.153951	77.84
30	2159.1	2034.03	-5.79292	-0.195625	77.9267
40	1190.8	1129.46	-5.15084	0.30719	78.035
50	732.58	698.666	-4.62941	-0.13521	78.1
60	485.86	468.989	-3.47243	-0.680227	78.36
80	248.57	242.252	-2.54189	-1.46951	78.36
100	145.46	143.133	-1.60006	-1.86576	78.36
150	53.437	53.7588	0.602201	-1.9105	78.36
200	25.943	26.5027	2.15755	-1.73646	78.36
300	9.4018	9.69475	3.11585	-2.33492	78.36
400	4.6561	4.74236	1.85264	-4.35333	78.36
500	2.7481	2.72657	-0.783425	-7.33465	78.36

Concerning the angular distribution of the Rayleigh scattering amplitudes, the dynamic screening model should provide lower values at low energies, especially for lighter elements, compared with the static screening model described in [10]. This may be noticed in Figs. 1–3.



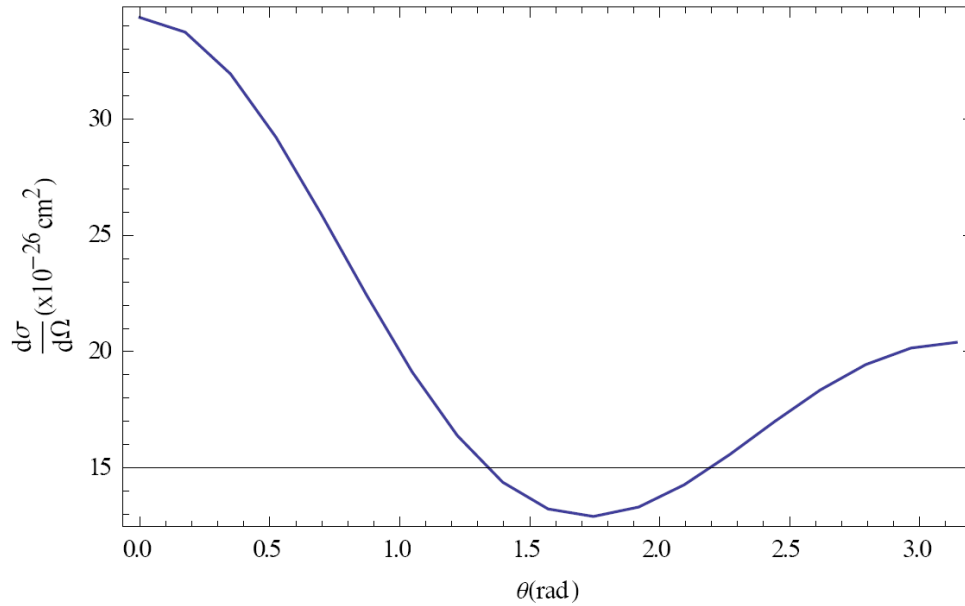


Fig. 1 – The angular distribution of the differential cross section of Rayleigh scattering on the 2s electrons of calcium for photon energy 6.04 keV.

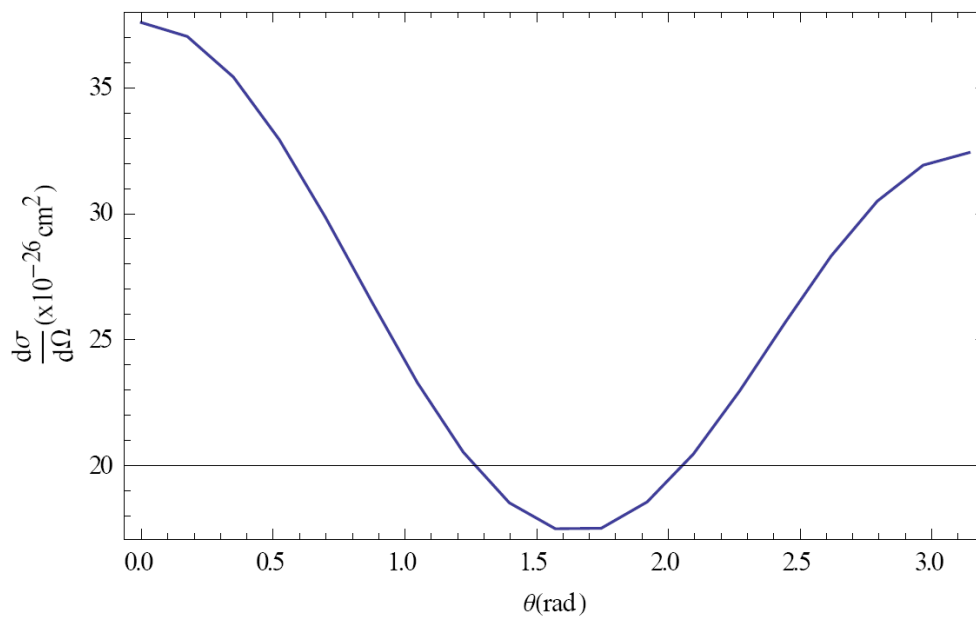


Fig. 2 – The angular distribution of the differential cross section of Rayleigh scattering on the 2s electrons of zinc for photon energy 6.04 keV.

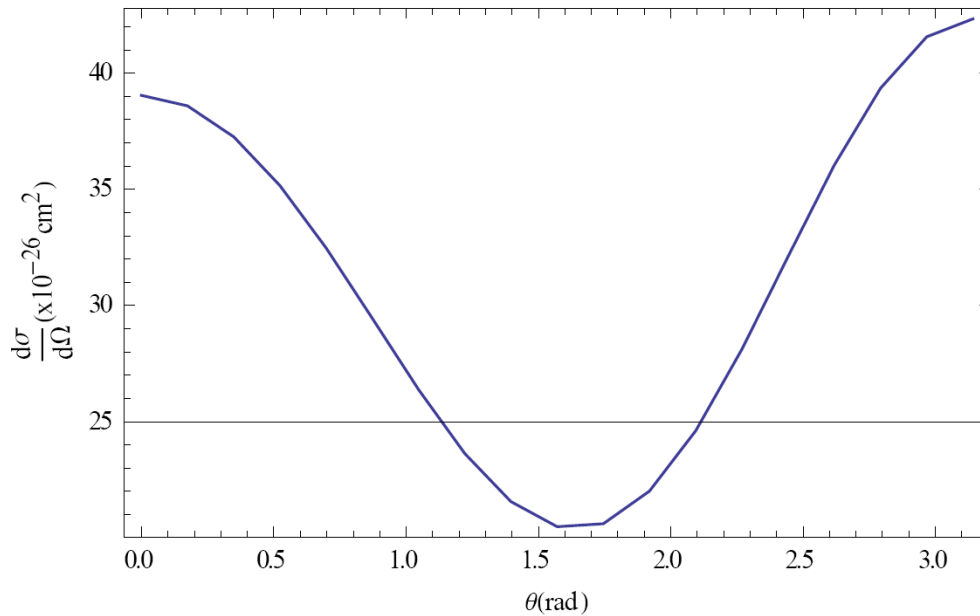


Fig. 3 – The angular distribution of the differential cross section of Rayleigh scattering on the  $2s$  electrons of silver for photon energy 10 keV.

### 3. CONCLUSIONS

As it may be noticed from the numerical results in the tables, the presented dynamic screening model considerably improves the predictions for the total photoeffect cross-section and hence for the angular distribution of the Rayleigh scattering on  $2s$  electrons in the case of low atomic number elements and energies closer to the photoeffect threshold. This proves that a coulomb field with an effective charge given by the Hartree-Fock method gives fairly good predictions both for Rayleigh scattering and photoeffect in a large energy range for any atomic number elements.

*Acknowledgements.* We wish to thank to Prof. A. Costescu for suggesting this work and many helpful discussions.

The work was partially supported by the Romanian Executive Unit for Financing Higher Education, Research and Inovation (UEFISCDI), under grant PN II 22-139/2008.

The work of C. Stoica was supported by the strategic grant POSDRU/89/1.5/S/58852, Project "Postdoctoral programme for training scientific researchers" cofinanced by the European Social Found within the Sectorial Operational Program Human Resources Development 2007–2013.

## REFERENCES

1. Y. Ding et al., Phys. Rev. Lett., **102**, 254801 (2009).
2. L. Young et al., Nature, **466**, 56 (2010).
3. N. Berrah et al., J. Mod. Opt., **57**, 1015 (2010).
4. P. M. Bergstrom Jr., T. Suric, K. Pisk and R.H. Pratt, Phys. Rev. A, **61**, 1134 (1993).
5. P.P. Kane P.P., Phys. Rep., **218**, 67 (1992).
6. A. N. Hoperski, I.D. Petrov, A.N. Nadolinski, V.A. Yavna and R. V. Koneev, J. Phys. B: At., Mol., Opt. Phys., **37**, 3313 (2004).
7. A. Costescu, S. Spanulescu, Phys. Rev. A, **73**, 022702 (2006).
8. A. Costescu, S. Spanulescu and C. Stoica, J. Phys. B: At., Mol., Opt. Phys., **40**, 2995 (2007).
9. Hoperski A.N., Nadolinsky A. M., Dzuba D.V. and Yavna V.A., J. Phys B: At. Mol. Opt. Phys., **38**, 1507 (2005).
10. A. Costescu et al., J. Phys. B: At. Mol. Opt. Phys., **44**, 045204 (2011).
11. A. Costescu et al., Rom. Rep. Phys., **63**, 782 (2011).
12. J. H. Scofield Lawrence, Radiation Laboratory Report No CRL 51326 (Livermore,CA, 1973), unpublished.
13. L. Kissel, <http://adg.llnl.gov/Research/scattering/>